

## Article

# Modifying Thermostability and Reusability of Hyperthermophilic Mannanase by Immobilization on Glutaraldehyde Cross-Linked Chitosan Beads

Beenish Sadaqat <sup>1,2</sup>, Chong Sha <sup>2</sup>, Mudasir Ahmad Dar <sup>2</sup>, Maruti J. Dhanavade <sup>3</sup>, Kailas D. Sonawane <sup>4</sup>, Hassan Mohamed <sup>1,5</sup>, Weilan Shao <sup>2,\*</sup> and Yuanda Song <sup>1,\*</sup>

<sup>1</sup> Colin Ratledge Center for Microbial Lipids, School of Agriculture Engineering and Food Science, Shandong University of Technology, Zibo 255049, China; beenish@sdut.edu.cn (B.S.); hassanmohamed85@azhar.edu.eg (H.M.)

<sup>2</sup> School of the Environment and Safety Engineering, Biofuels Institute, Jiangsu University, Zhenjiang 212013, China; jnshachong@163.com (C.S.); mudasir.dar@unipune.ac.in (M.A.D.)

<sup>3</sup> Department of Microbiology, Bharati Vidyapeeth's Dr Patangrao Kadam Mahavidyalaya College, Sangli 416416, India; marutijd@gmail.com

<sup>4</sup> Structural Bioinformatics Unit, Department of Biochemistry, Shivaji University, Kolhapur 416004, India; kds\_biochem@unishvaji.ac.in

<sup>5</sup> Department of Botany and Microbiology, Faculty of Science, Al-Azhar University, Assiut 71524, Egypt

\* Correspondence: weilanshao@foxmail.com (W.S.); ysong@sdut.edu.cn (Y.S.)

**Abstract:** In the current study, the purified  $\beta$ -mannanase (Man/Cel5B) from *Thermotoga maritima* was immobilized on glutaraldehyde cross-linked chitosan beads. The immobilization of Man/Cel5B on chitosan beads was confirmed by Fourier-transform infrared spectroscopy (FTIR) and X-ray diffraction (XRD) analysis. After immobilization, the protein loading efficiency and immobilization yield were found to be 73.3% and 71.8%, respectively. The optimum pH for both free and immobilized enzymes was found to be pH 5.5. However, the optimum temperature of immobilized Man/Cel5B increased by 10 °C, from 85 °C (free Man/Cel5B) to 95 °C (Immobilized). The half-life of free and immobilized enzymes was found to be 7 h and 9 h, respectively, at 85 °C owing to the higher thermostability of immobilized Man/Cel5B. The increase in thermostability was also demonstrated by an increase in the energy of deactivation (209 kJmol<sup>-1</sup>) for immobilized enzyme compared to its native form (92 kJmol<sup>-1</sup>), at 85 °C. Furthermore, the immobilized Man/Cel5B displayed good operational stability as it retained 54% of its original activity after 15 repeated catalytic reactions concerning its free form.

**Keywords:**  $\beta$ -mannanase; docking; hyperthermostable; kinetics



**Citation:** Sadaqat, B.; Sha, C.; Dar, M.A.; Dhanavade, M.J.; Sonawane, K.D.; Mohamed, H.; Shao, W.; Song, Y. Modifying Thermostability and Reusability of Hyperthermophilic Mannanase by Immobilization on Glutaraldehyde Cross-Linked Chitosan Beads. *Biomolecules* **2022**, *12*, 999. <https://doi.org/10.3390/biom12070999>

Academic Editor: Tigran Chalikian

Received: 23 June 2022

Accepted: 12 July 2022

Published: 18 July 2022

**Publisher's Note:** MDPI stays neutral with regard to jurisdictional claims in published maps and institutional affiliations.



**Copyright:** © 2022 by the authors. Licensee MDPI, Basel, Switzerland. This article is an open access article distributed under the terms and conditions of the Creative Commons Attribution (CC BY) license (<https://creativecommons.org/licenses/by/4.0/>).

## 1. Introduction

Mannans are an integral part of hemicellulose and are predominantly found in the soft woods, plant endosperms, seeds, and vacuoles of a wide variety of plants [1–3]. Mannans are also present as glycoproteins in the cell walls of some yeasts, fungi, and bacteria [4].  $\beta$ -1,4-mannanase (mannan mannohydrolase, EC 3.2.1.78) is an endo-acting hydrolase that randomly cleaves the  $\beta$ -1,4-mannosidic linkages in the main chain of mannans (linear mannan, galactomannan, glucomannan, and galactoglucomannan), therefore producing manno oligosaccharides (MOS) of various lengths [5].  $\beta$ -mannanase has wide industrial applications as it is used for the production of partially hydrolyzed guar gum, MOS, fruit juice clarification, paper/pulp bio-bleaching, synthesis of detergents, amelioration of animal or poultry feed, and saccharification of biomass [6,7].

Despite the versatility of  $\beta$ -mannanase, the use of these enzymes in soluble form at the industrial scale has some limitations including low stability, unmanageable recovery and reuse, short shelf life, difficulty in handling, and loss of activity at prolonged operational

conditions [8]. However, immobilization of enzymes on or into solid matrixes can address these issues. It should be noted that immobilization may not always bring desirable changes to the enzyme system. The immobilization protocol must consider several aspects, such as properties of support material, the active group of the support used to immobilize the enzyme and that of the enzyme molecule, and the immobilization protocol used. Only a proper selection of these three aspects allows one to take full advantage of the immobilization process [9].

Immobilization can enhance the thermostability, pH stability, functional stability, and affinity of these biocatalysts [10]. In addition to this, immobilization enables easy recovery of biocatalysts from the end product and provides opportunities for scaling up and enabling the development of processes based on different reactor configurations and reduction of operating costs [11]. Previously,  $\beta$ -mannanases have been immobilized on different support materials which include sodium alginate-grafted  $\beta$ -cyclodextrin [12], chitosan magnetic nanocomposites [13], cross-linked enzyme aggregates [14], and calcium alginate beads [15].

The efficiency of immobilization largely depends on the interaction of enzyme and support matrix. Therefore, the type of immobilization matrix plays a very important role in deciding the characteristics of the resultant immobilized biocatalysts [16]. The immobilization process may be of a physical nature, which includes adsorption, entrapment, and encapsulation of enzyme on or inside support matrix [17] or it may be of chemical nature which involves crosslinking and covalent bonding [18]. Numerous inert materials could be used for effective immobilization of enzymes because of their ability to reuse, easy recovery, higher thermal stability, and ability to survive under varying pH conditions [19]. Chitosan is one of the most widely used support materials for enzyme immobilization because of unique properties such as the presence of a large number of functional groups, ease of availability, biodegradability, and chemical resistance [20]. Chitosan beads have been widely used for the immobilization of  $\beta$ -mannanase which resulted in enhanced activity, stability, and reusability of enzyme. The presence of amino groups in chitosan structure also allows modification by crosslinking process. Glutaraldehyde is the most frequently used crosslinking agent which can further enhance rigidity, thermal stability, and absorptivity of chitosan support material. The covalent immobilization of enzyme on chitosan occurs by treating it with glutaraldehyde crosslinker. The bifunctional  $-CHO$  groups of glutaraldehyde react with the  $-NH_2$  groups present in chitosan and in the enzyme [21]. Işık et al. [22] used glutaraldehyde cross-linked chitosan beads for covalent immobilization of acetylcholinesterase (AChE) enzyme which resulted in high stability and reusability of enzyme.

In the current study, hyperthermostable  $\beta$ -mannanase from *T. maritima* (Man/Cel5B); which was purified and characterized in a previous study [6]; was immobilized on glutaraldehyde cross-linked chitosan beads. Properties of the immobilized and free Man/Cel5B were compared. Moreover, the kinetic and thermodynamic parameters of both forms of the Man/Cel5B were determined by applying different statistical tools to predict and compare their behavior under different environmental conditions. Finally, the interactions between ligand and the Man/Cel5B were studied using *in silico* structure-based molecular docking methods.

## 2. Materials and Methods

### 2.1. Chemicals

Chitosan (average molar weight,  $4.9 \times 10^5$ , degree of deacetylation 95%), locust bean gum (LBG), and glutaraldehyde ( $\geq 98\%$  purity) were purchased from Sigma Chemical Co. (St. Louis, MO, USA). All other chemicals were of analytical grade and were purchased from Sinopharm Chemical Reagent Co. Ltd. (Shanghai, China).

### 2.2. Chitosan Beads Preparation and Immobilization of Man/Cel5B

Chitosan beads were prepared according to the procedure described by Kaushal [23] with slight modifications. Briefly, 2.5 g of chitosan was dissolved in 100 mL of 1% (*v/v*)

acetic acid solution using continuous stirring till the solution was clear from any solids. The chitosan solution was added dropwise into 2% (*w/v*) of NaOH solution and beads were collected from precipitating solution. The prepared beads were placed in 100 mL of crosslinking solution for almost 3 h at 25 °C. The crosslinking solution was prepared by adding 0.2 vol.% of glutaraldehyde to 100 mL of the ddH<sub>2</sub>O. The crosslinked beads were filtered and stored at 4 °C for future use. The beads were lyophilized and surface morphology was observed using scanning electron microscopy on a SEM, Quanta FEG 250 machine [24].

For immobilization of Man/Cel5B onto chitosan beads, 1 mL of Man/Cel5B (purified near homogeneity in previous study) [6] was mixed with 9 mL of PI buffer (pH 6.8) and added to approximately 15 g of crosslinked chitosan beads previously stored at 4 °C. The cross-linked chitosan beads were placed in an enzyme solution (0.364 mg/mL) for 5 h at 30 °C in a rotary shaking incubator. The beads were then washed with cold phthalate-imidazole (PI; pH 6.8) buffer and stored at 4 °C for future use.

### 2.3. Activity of Immobilized Man/Cel5B Enzyme

The activity of immobilized Man/Cel5B was determined via 4-hydroxybenzoic acid hydrazide method [25]. The reaction mixture, containing 0.2 g of immobilized Man/Cel5B chitosan beads, 100 µL of 0.5% (*m/v*) LBG as substrate, and 100 µL of 0.25 M PI buffer (pH 5.5); was incubated for 5 min at the target temperature (e.g., 60–95 °C for evaluation of optimum temperature). The beads were removed, and 600 µL of stop solution was immediately added to stop the reaction. For free enzyme, 100 µL of Man/Cel5B was added to the reaction mixture instead of 0.2 g of beads. The mixture was boiled for 10 min and the absorbance was measured at 405 nm after cooling the reaction mixture on ice (0 °C). One unit of enzyme is the amount that produced 1 µmol of mannose sugar per minute under the said assay conditions [21].

### 2.4. Estimation of Protein Loading and Immobilization Yield

The total protein concentration was determined by measuring the absorbance at 280 nm [26]. The total amount of protein that immobilized on chitosan beads was estimated by subtracting the total protein concentration of supernatant (after immobilization of beads) from the protein concentration of free enzyme. In this regard, protein loading efficiency (%) and immobilization yield (%) were calculated by the following equations:

$$\text{Protein Loading efficiency (\%)} = \frac{\text{Total amount of immobilized enzyme}}{\text{Total amount of initial enzyme}} \times 100 \quad (1)$$

$$\text{Immobilized yield (\%)} = \frac{\text{Specific activity of immobilized enzyme}}{\text{Specific activity of free enzyme}} \times 100 \quad (2)$$

### 2.5. Biochemical Characterization of Immobilized Man/Cel5B

#### 2.5.1. Effect of Temperature on Immobilized Man/Cel5B Activity

The impact of temperature on immobilized enzyme was verified by determining the enzyme activity at a temperature ranging from 60 to 100 °C with a temperature difference of 5 °C. The reaction set showing the highest enzyme activity was considered as 100% activity and the relative activity was determined concerning the maximum enzyme activity. The activation energy ( $E_{\text{act}}$ ) was evaluated from the slope of Arrhenius plot ( $\ln$  of % relative activity versus  $1000/\text{absolute temperature}$ ) using the following equation:

$$E_{\text{act}} = -\text{slope} \times R \quad (3)$$

where  $R$  is the gas constant ( $8.314 \text{ J}\cdot\text{K}^{-1} \text{ mol}^{-1}$ ), and  $E_{\text{act}}$  represents activation energy ( $\text{kJ}\cdot\text{mol}^{-1}$ ). The impact of temperature on free enzyme was also determined using same conditions and compared with the immobilized enzyme

### 2.5.2. Effect of pH on Enzyme Activity

The optimum pH for both free and immobilized enzyme was examined at pH ranging from pH 4.0 to 7.5, using 25 mM PI buffer at the optimal temperature. The reaction set showing the highest enzyme activity was taken as 100% activity, and the relative activity was determined concerning the maximum enzyme activity.

### 2.5.3. Kinetics and Thermodynamics of Substrate Hydrolysis

The kinetic parameters of free and immobilized enzymes were calculated by observing the activity in increasing substrate concentration i.e., 0.5–15.0 mg/mL. The activity was evaluated at the optimum temperature and pH. The Michaelis–Menten constant ( $K_m$ ) and maximum rate of reaction ( $V_{max}$ ) were determined using the Michaelis–Menten ( $V$  vs.  $[S]$ ) and Lineweaver–Burk plots ( $1/V$  vs.  $1/[S]$ ). The turnover number ( $k_{cat}$ ) was calculated by the equation given below:

$$k_{cat} = V_{max} / [E_t] \quad (4)$$

where  $E_t$  is the total enzyme concentration.

The thermodynamic parameters, change in enthalpy ( $\Delta H$ ), change in entropy ( $\Delta S$ ), and Gibb's free energy ( $\Delta G$ ) were used to understand the behavior of enzymatic reactions and interactions and were calculated by the equations given below:

$$\Delta H = E_{act} - RT \quad (5)$$

where  $R$  is the gas constant,  $T$  is the absolute temperature and  $E_{act}$  is the activation energy.

$$\Delta G = -RT * \ln (k_{cat} \times h / k_B * T) \quad (6)$$

where  $h$  is the Planck constant ( $6.626 \times 10^{-34}$  J s), and  $k_B$  is the Boltzmann constant ( $1.38 \times 10^{-23}$  J·K<sup>-1</sup>).

$\Delta S$  was calculated using the following equation:

$$\Delta S = (\Delta H - \Delta G) / T \quad (7)$$

### 2.5.4. Thermostability of Immobilized Enzyme and Kinetics of Enzyme Denaturation

Thermostability was determined by incubating the immobilized enzyme and free enzyme at 85 °C, 90 °C, and 95 °C for 5 h. Samples were taken after each hour and the residual activity was calculated at optimum temperature and pH. Enzyme activity without incubation of the enzyme at optimum conditions was taken as 100%. The data were fitted to a pseudo-first-order plot and inactivation rate constants ( $k_d$ ) were calculated at each temperature. The half-life ( $t_{1/2}$ ) of the enzyme at each temperature was calculated by the equation:

$$t_{1/2} = \ln 2 / k_d \quad (8)$$

where  $k_d$  was calculated from the slope of the graph plotted between  $-\ln$  of  $E/E_i$  ( $E_i$  is the initial enzyme activity and  $E$  is the enzyme activity at time  $t$ ). The energy of activation for irreversible inactivation ( $E_d$ ) of the enzyme was determined by the Arrhenius plot that was plotted as  $\ln k_d$  versus  $1000/T$ .

The  $\Delta H_d$ ,  $\Delta G_d$ , and  $\Delta S_d$  of irreversible inactivation of both free and immobilized Man/Cel5B were calculated by applying Equations (5)–(7) with the modifications that in Equation (5)  $E_d$  was used instead of  $E_{act}$  and in Equation (6)  $k_d$  was used instead of  $k_{cat}$ .

### 2.6. Reusability of Immobilized Beads

The reduction in enzyme activity of immobilized Man/Cel5B after each use was tested as described in Section 2.3. To remove any left-out substrate, the beads were removed and washed by PI buffer (pH 6.8) after each experimental run. The washed beads were mixed with fresh substrate and the residual activity was measured at optimum conditions.

### 2.7. Analysis of Chitosan and Enzyme Immobilized Chitosan Beads

The FTIR spectrum of immobilized chitosan beads was recorded from 4000 to 400  $\text{cm}^{-1}$ ; using a Bruker FTIR spectrophotometer (ALPHA II Bruker) equipped with a platinum ATR sampling module and compared to the FTIR spectrum of chitosan beads without immobilization of the enzyme. Both chitosan beads and enzyme immobilized beads were lyophilized before processing for the FTIR spectrum analysis.

The crystallographic structure of chitosan and immobilized chitosan beads was determined using X-ray diffraction analysis (XRD). The XRD pattern was analyzed using Bruker D8 advance X-ray diffractometer at room temperature from 10° to 50° with a scan speed of 0.08°/s.

### 2.8. Molecular Docking Study

The homology modeling of Man/Cel5B was carried out with a SWISS-MODEL homology program [27]. The obtained model was validated by VERIFY-3D [28] and the Phi/Psi Ramachandran plot was acquired from the PROCHECK analysis tool [29]. The active sites present in the 3D model were predicted using the CASTp online server. The 3D structure of mannotriose was built in the Sybyl software package (Version 7.1, Tripos, Inc., St. Louis, MO, USA). Then the molecular docking of Man/Cel5B and mannotriose was performed by AutoDock software (Version 4.2, Merck & Co.GPL, Kenilworth, NJ, USA). The final structure obtained after the molecular docking studies were analyzed with the structural visualization software programs CHIMERA (Version 1.15, RBVI, UCSF, San Francisco, CA, USA) [30] and Discovery Studio Visualizer (Version 4.1, Dassault Systemes, Waltham, MA, USA) [31].

### 2.9. Statistical Analysis

All the experiments were accomplished in triplicate and the results were reported as the arithmetic mean  $\pm$  standard deviation (SD). Analysis of variance (ANOVA) of data was performed with SPSS software version 22 (IBM SPSS, Armonk, NY, USA) statistical software using one-way analysis of variance, using the Tukey similarity test.  $p$  values  $< 0.05$  were considered statistically significant and indicated with “\*” in figures.

## 3. Results and Discussion

### 3.1. Surface Morphology of Chitosan Beads

The chitosan beads were synthesized successfully when chitosan dissolved in acetic acid was slowly dropped in NaOH solution. However, the continuous and protracted exposure may soften or disintegrate these beads. Therefore, the beads were further modified by cross-linking amine groups present in chitosan with glutaraldehyde by the establishment of the Schiff base imine bonds [32]. The beads were spherical and white in appearance. The SEM revealed that the beads were coarsely circular in shape and the surface of the beads was rough (Figure 1). The Man/Cel5B was immobilized on the prepared cross-linked beads for 5 h under shaking conditions, which resulted in 71.8% protein immobilization yield which is an important parameter to determine the percentage of enzyme that has been immobilized on or inside the solid matrix. The immobilization of thermophilic trehalose synthase on chitosan activated with glutaraldehyde by Kim et al. [33] resulted in 38% immobilization yield. Dincer et al. [34] observed 67% immobilization yield when tyrosinase was immobilized on chitosan-clay composite beads. Dhiman et al. [12] immobilized  $\beta$ -mannanase on sodium alginate-grafted- $\beta$ -cyclodextrin, which resulted in 91.5% immobilization yield. This suggests that the enzyme leakage in our study was higher compared to study by Dhiman et al. [12], which could be improved in the future studies. The protein loading efficiency of Man/Cel5B was found to be 73.3% which was almost similar to the protein loading efficiency (78.4%) observed by Kaushal et al. [23] when catalase was immobilized on glutaraldehyde cross-linked chitosan beads.



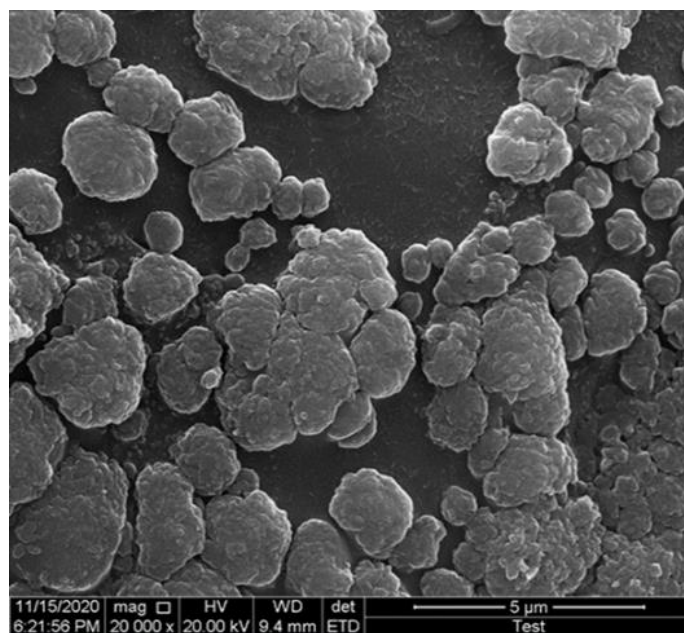


**Figure 1.** SEM micrograph of glutaraldehyde cross-linked chitosan beads.

### 3.2. Biochemical Characterization of Free and Immobilized Enzyme

#### 3.2.1. Effect of Temperature on Man/Cel5 B Immobilized Enzyme

The temperature dependence of free and immobilized Man/Cel5B was studied between 60 and 95 °C. The optimum temperatures of free and immobilized Man/Cel5B were found to be 85 °C and 95 °C, respectively (Figure 2). The immobilized enzyme was therefore further characterized at 100 °C, where it showed a sharp decline in activity. The optimum temperature of the immobilized Man/Cel5B was enhanced by 10 °C which reveals that the rigidity of Man/Cel5B increased after immobilization [35]. Similarly, the optimum temperature of  $\alpha$ -amylase from *Vigna radiata*; increased by 10 °C upon immobilization on chitosan beads [36]. The activity of the free enzyme dropped significantly when the temperature increased from 85 °C to 90 °C. Nevertheless, the activity of the immobilized enzyme continuously increased to 95 °C, which reveals that the support provides protecting effect to the enzyme at higher temperatures [37]. A similar effect of immobilization on enzymes was also observed previously [35]. The possible reason for increased optimum temperature of immobilized enzyme may be because of the synergic effect between enzyme and chitosan beads. In addition, the immobilized matrix may be able to provide a suitable micro-environment at an active center for enzyme and substrate interaction and keep its rigid confirmation and function, especially at higher temperatures [38]. However, the extent of effect varies for different support materials used and with the type of interaction established between enzyme and the solid support.

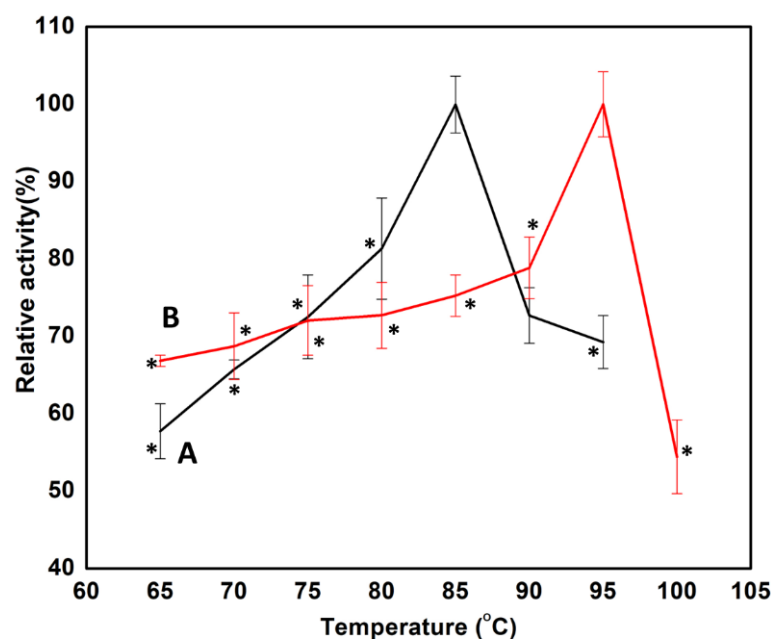


**Figure 2.** Effect of temperature on the free and immobilized Man/Cel5B activity. (A) Free Man/Cel5B. The temperature values showing significant ( $p < 0.05$ ) difference from optimum temperature were marked with “\*”. (B) Immobilized Man/Cel5B. The temperature values showing significant ( $p < 0.05$ ) difference from optimum temperature were marked with “\*”.

### 3.2.2. Kinetic Parameters of Free and Immobilized Enzyme

The kinetic parameters of both free and immobilized enzymes were analyzed by changing the concentration of substrate (LBG) from 0.5 mg/mL to 15 mg/mL. The  $K_m$  values of free and immobilized Man/Cel5B were found to be 10.7 mg/mL and 4.8 mg/mL, respectively, from Lineweaver-Burk Plots (Figure 3). The result indicates that immobilized Man/Cel5B with a lower  $K_m$  value has significantly higher affinity for the substrate in comparison to the free enzyme. Possibly, the Man/Cel5B expanded on the surface of chitosan beads with a better orientation which resulted in more available active sites for substrate binding that eventually causes higher affinity and lower  $K_m$  value. The decrease in the  $K_m$  value after immobilization is a desirable property and many authors reported significant decrease in  $K_m$  after immobilization of the enzymes. The decrease in  $K_m$  value could be due to increased availability of substrate molecule to the active site of the enzyme molecule [39]. When the enzyme was immobilized on silica-coated modified magnetite nanoparticles, the  $K_m$  value of  $\alpha$ -Amylase decreased from 6.3 mM to 4.8 mM [39]. Similarly, the  $K_m$  value of  $\alpha$ -Amylase decreased after immobilization on bioactive phospho-silicate glass [40].

Furthermore, the  $V_{max}$  of free and chitosan immobilized Man/Cel5B was found to be  $106 \mu\text{mol} (\text{min mg protein})^{-1}$  and  $2.56 \mu\text{mol} (\text{min mg protein})^{-1}$ , respectively. The decrease in the  $V_{max}$  was also observed by Çetinus and Oztop [41] when catalase was immobilized on chitosan beads. The  $V_{max}$  of beta-mannanase immobilized on Na-alginate- $\beta$ CD was also lower than the free enzyme [12]. Although higher  $V_{max}$  after immobilization is a desirable property, the reason for  $V_{max}$  being lower than the free enzyme system could be because of the conformational changes in the enzyme after immobilization on the support material. Another reason may be seepage or congestion of the enzyme during the adsorption process of adsorbate-adsorbent interaction [12]. These parameters should be better optimized in future studies.

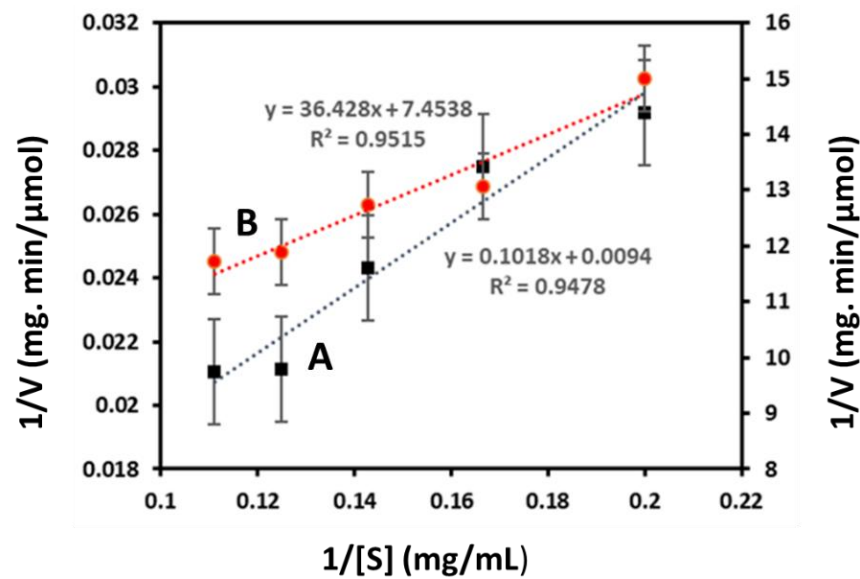


**Figure 3.** Lineweaver-Burk plots of free and immobilized Man/Cel5B. (A) Free Man/Cel5B (B) Immobilized Man/Cel5B.

### 3.2.3. Thermodynamics of LBG Hydrolysis

The calculated activation energy ( $E_{act}$ ) of free and immobilized enzymes from Arrhenius plots (Figure 4) depicted a reduction from 26.34 J/mol to 6.64 J/mol (Table 1). Similarly, the  $E_{act}$  of  $\beta$ -mannanase decreased from 28.19 kJmol<sup>-1</sup> to 23.52 kJmol<sup>-1</sup> after immobilization on sodium-alginate-grafted- $\beta$ -cyclodextran [12]. A similar observation was also reported when mannanase from *P. chrysogenum* was immobilized by entrapment on calcium alginate beads [42]. The decrease in  $E_{act}$  indicates that immobilized enzyme requires less energy to overcome the barrier for conversion of substrate into product. This conceivably means that the immobilization process saves energy which makes the immobilized enzyme more valuable economically: a vital advantage for industrial use of the enzyme [12]. The decrease in the activation energy also indicated a lower sensitivity to the temperature and higher affinity for the active site of the immobilized enzyme [43].

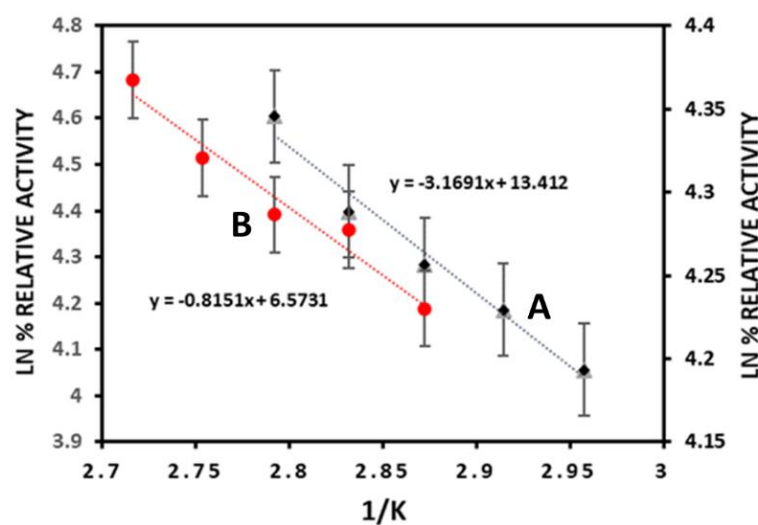


**Figure 4.** Arrhenius plots for free and immobilized Man/Cel5B. (A) Free Man/Cel5B (B) Immobilized Man/Cel5B.



**Table 1.** Thermodynamic parameters of immobilized and free enzyme for LBG degradation.

Thermodynamic Parameter	Immobilized Enzyme	Free Enzyme
$E_{act}$ (KJmol <sup>-1</sup> )	6.78 ± 0.88	26.35 ± 3.33
$\Delta H$ (KJmol <sup>-1</sup> )	3.72 ± 0.26	23.37 ± 2.68
$\Delta G$ (KJmol <sup>-1</sup> )	85.17 ± 3.26	72.68 ± 4.21
$\Delta S$ (J·mol <sup>-1</sup> ·K <sup>-1</sup> )	−221.33 ± 5.13	−137.74 ± 4.49

The thermodynamic parameters  $\Delta H$ ,  $\Delta G$ , and  $\Delta S$  were also calculated and the results are shown in Table 1. The  $\Delta H$  for free and immobilized enzymes were found to be 23.37 KJ/mol and 3.72 KJ/mol, respectively. The decrease in enthalpy value demonstrates that the formation of the enzyme-substrate complex was more efficient for the immobilized Man/Cel5B compared to the free enzyme [44]. The  $\Delta G$  for the immobilized enzymes was found to be 85.26 KJ/mol which was slightly higher than the  $\Delta G$  observed for the free enzyme, which is 72.68 KJ/mol. The increase in  $\Delta G$  indicates that conversion of substrate-enzyme transition complex was more spontaneous for the free enzyme compared to the immobilized enzyme. The  $\Delta S$  for immobilized and free enzymes were found to be −221.33 J/mol/K and −137.74 J/mol/K, correspondingly. The lower value of  $\Delta S$  indicates a lesser disorder for the transition complex of the immobilized enzyme system [45].

#### 3.2.4. Thermostability of Free and Immobilized Man/Cel5B

The immobilized and free Man/Cel5B were incubated at 85 °C, 90 °C, and 95 °C. The results (Figure 5) clearly show that thermostability increased after immobilization of Man/Cel5B on chitosan beads. The enzyme was able to retain >65% of its initial activity after 5 h of incubation at 85 °C compared to 55% of the free enzyme. At higher temperatures, the free enzyme lost activity more rapidly compared to the immobilized enzyme. These results suggest that the free enzyme was exposed to conformational changes as the temperature of reaction system increased, which resulted in rapid denaturation of enzyme and consequently loss of activity. However, for immobilized enzyme the interaction between support and enzyme provides more stable conformation which protects the immobilized enzyme at higher temperatures [46]. The immobilized enzyme retained more than 60% and 50% of activity after 5 h of incubation at 90 °C and 95 °C, respectively. However, the free enzyme could only retain 49% and 26% of initial enzyme activity after 5 h at 90 °C and 95 °C, respectively. The extent of thermal inactivation was determined using Pseudo-first-order plots, and thermal inactivation constants ( $k_d$ ) were calculated for both types of enzyme systems. The  $k_d$  values (Table 2) were found to be 0.074/h, 0.079/h and 0.106/h for immobilized; and 0.097/h, 0.11/h, and 0.22/h at 85, 90 and 95 °C respectively. Similarly, the  $k_d$  values of lipase immobilized on sol-gel decreased from 0.02/h to 0.01/h [47]. The decrease in  $k_d$  indicates higher stability of enzyme at elevated temperatures which suggests that immobilization protected the tertiary structure of enzyme by preventing denaturation [46]. The decimal reduction time (D-value) of immobilized Man/Cel5B increased to 1864, 1742 and 1403 from 1424, 1244, 611 at 85, 90 and 95 °C, respectively. This may be because of the formation of multiple covalent bonds between enzyme and crosslinked chitosan beads, which result in a reduction of conformational flexibility and thermal vibration; accordingly protein unfolding and denaturation were prevented [48]. Moreover, the half-life ( $t_{1/2}$ ) of the enzyme considerably increased after immobilization, which was found to be 9 h for the immobilized enzyme compared to only 7 h for the free enzyme at 85 °C (Table 2). The half-life of both free and immobilized enzymes decreased at higher temperatures; however, the half-life of the immobilized enzyme was found to be higher than the free enzyme also at higher temperatures. The increased half-life of the immobilized enzyme complex indicates high thermal stability of the immobilized Man/Cel5B. Altun et al., also observed increase in the thermostability of pepsin after immobilization on chitosan beads [43]. The structural rigidity and heat resistance of the enzyme can increase to a great extent after attachment to a suitable support [49]. This

results in the decreased sturdiness of free enzymes compared to immobilized enzyme at same temperatures [50].

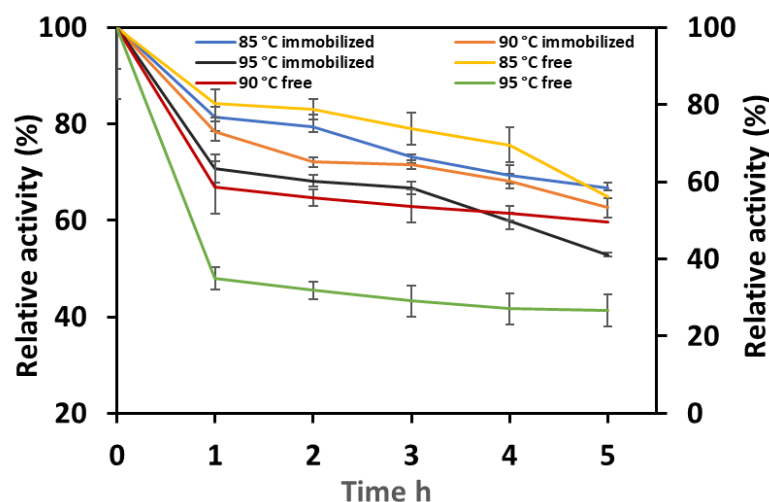


**Figure 5.** Thermostability of free and immobilized Man/Cel5B. The enzymes were incubated at 80, 85 and 90 °C for 5 h in the absence of substrate, and the residual activity was examined at optimal conditions.

**Table 2.** Thermodynamic parameters for irreversible inactivation of free and immobilized Man/Cel5B.

Parameter	Immobilized Enzyme			Free Enzyme		
	85	90	95	85	90	95
$K_d$ ( $\text{min}^{-1}$ )	$4.45 \pm 0.03$	$4.75 \pm 0.99$	$6.63 \pm 1.23$	$5.82 \pm 0.42$	$6.66 \pm 0.24$	$13.5 \pm 0.44$
$t_{1/2}$ ( $\text{min}^{-1}$ )	$561 \pm 2.12$	$524 \pm 3.30$	$392 \pm 3.63$	$428 \pm 1.35$	$374 \pm 2.63$	$184 \pm 3.33$
D-value	$1864 \pm 8.53$	$1742 \pm 4.12$	$1303 \pm 1.67$	$1424 \pm 3.33$	$1244 \pm 6.55$	$611 \pm 5.45$
$\Delta H_d$ ( $\text{KJmol}^{-1}$ )	$206.24 \pm 2.04$	$206.20 \pm 2.85$	$206.16 \pm 1.35$	$89.41 \pm 2.45$	$89.37 \pm 1.84$	$89.33 \pm 2.63$
$\Delta G_d$ ( $\text{KJmol}^{-1}$ )	$82.80 \pm 1.48$	$84.00 \pm 2.43$	$85.20 \pm 1.67$	$72.71 \pm 1.64$	$73.77 \pm 2.50$	$74.82 \pm 8.46$
$\Delta S_d$ ( $\text{J}\cdot\text{mol}^{-1}\cdot\text{K}^{-1}$ )	$-230.63 \pm 1.90$	$-230.75 \pm 4.44$	$-230.87 \pm 3.24$	$-202.76 \pm 3.44$	$-202.89 \pm 1.53$	$-203.01 \pm 2.43$

### 3.2.5. Thermodynamics of Enzyme Stability after Immobilization

The  $E_d$  values for the free and immobilized Man/Cel5B were determined using Arrhenius plots (Figure 6) which were found to be  $92 \text{ KJmol}^{-1}$  and  $209 \text{ KJmol}^{-1}$ , respectively. The increase in  $E_d$  indicates that immobilized Man/Cel5B is more resistant to heat denaturation, therefore in need of excess energy as compared to the free enzyme [44], which is a desirable characteristic for industrial use of immobilized Man/Cel5B. The  $E_d$  is also related to another important thermodynamic parameter known as enthalpy of activation for thermal denaturation  $\Delta H_d$ . The value of  $\Delta H_d$  for immobilized Man/Cel5B was higher at all temperatures than the free Man/Cel5B (Table 2). The higher values of  $E_d$  and  $\Delta H_d$  indicate high thermal stability of the immobilized Man/Cel5B however, it is also important to note the values of  $\Delta G_d$  and  $\Delta S_d$ . As indicated in Table 2, the  $\Delta G_d$  values of the immobilized enzyme were higher than the free enzyme at all temperatures. The  $\Delta G_d$  values depict how favorable is the process of inactivation at a particular temperature. Lower  $\Delta G_d$  values of free enzyme indicate the process of thermal denaturation for the free enzyme is more spontaneous compared to immobilized enzyme complex. These results also suggest that interaction between support and enzyme provides more stable conformation which prevents the tertiary structure of enzyme from denaturation. The  $\Delta G_d$  values also depict higher thermal stability of immobilized enzyme than free Man/Cel5B which increases its value for industrial use. Furthermore, the lower  $\Delta S_d$  indicates a decrease in the degree of disorder for the immobilized enzyme system [51].

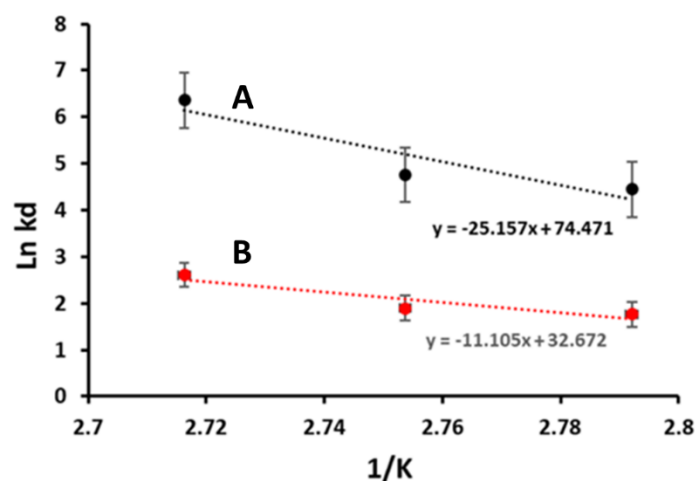


**Figure 6.** Arrhenius plots to calculate activation energy “ $E_d$ ” for irreversible thermal inactivation/denaturation of free and immobilized Man/Cel5B. (A) Free Man/Cel5B. (B) Immobilized Man/Cel5B.

### 3.2.6. Effect of pH on Free and Immobilized Man/Cel5B

The process of immobilization affects the ionization state, dissociation constant, and conformation of the enzyme. As a result, the relationship between pH, stability, and catalytic activity of the enzyme changes. To determine the effect of immobilization on the chemical characterization of the enzyme, the optimum pH of the immobilized enzyme was compared with the free Man/Cel5B (Figure 7). The effect of pH was determined in the range of pH 4–7 using PI buffer at optimum temperature (85 °C and 95 °C for free and immobilized enzyme, respectively). The optimum pH for both forms of Man/Cel5B enzyme was found to be pH 5.5. The chitosan beads may become disintegrated in acidic medium after long experimental exposures. In a study carried out by Worthen et al. [52] chitosan beads remained unchanged after the first seven hours at pH 5; however, the beads started to slowly shrink after 8 h and were almost disintegrated after 16 h of exposure to pH 5. However, in the current study, the immobilized enzyme showed the optimum activity at pH 5.5, which should be examined in the future studies. Additionally, it may be possible that crosslinking enhances the pH stability of chitosan beads, which was also observed by Worthen et al. [52], when chitosan beads were crosslinked by Tripolyphosphate. However, the effect of glutaraldehyde must be explored in future studies. The immobilized enzyme depicted enhanced activity in the pH range of 5.5–7. This enhanced activity of immobilized enzyme toward neutral pH may be as a result of the covalent binding of the enzyme with chitosan and change in the immediate microenvironment of the enzyme [8]. Our observations were in congruence with the findings of Mohapatra et al., who demonstrated no change in the optimum pH of  $\beta$ -mannanase from *Streptomyces* spp. Alg-S25 after immobilization on chitosan nanoparticles [53]. Similarly, the optimum pH of bovine liver catalase upon immobilization on chitosan beads was found to be same as its native form [8]. However, there are many reports where the optimum pH of the enzyme shifted after immobilization on the chitosan beads. For example, the optimum pH of  $\beta$ -mannanase from *Penicillium occitanis* decreased to pH 3 from pH 4 when the enzyme was immobilized on chitosan bentonite beads [54]. This shows that different enzymes do behave differently to the change in pH of the immediate environment when immobilized on chitosan beads.

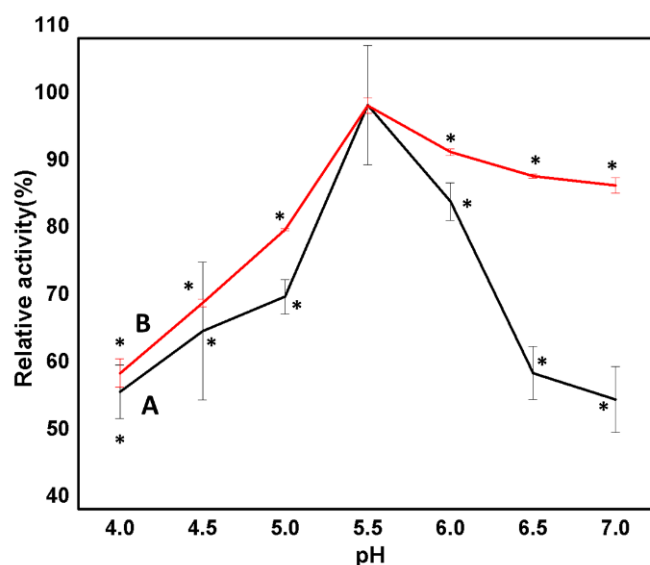


**Figure 7.** Effect of pH on the free and immobilized Man/Cel5B activity. (A) Free Man/Cel5B. The pH values showing significant ( $p < 0.05$ ) difference from optimum pH were marked with “\*”. (B) Immobilized Man/Cel5B. The pH values showing significant ( $p < 0.05$ ) difference from optimum pH were marked with “\*”.

### 3.3. Reusability of Immobilized Man/Cel5B

The reusability of immobilized enzymes is an important parameter from the economical point of view, as well as for the industrial use of enzymes. The reusability of immobilized Man/Cel5B was evaluated 15 times at the optimum temperature and pH (Figure 8). The immobilized enzyme showed excellent reusability as it retained almost 85% of the initial activity after the first cycle. The enzyme started losing its activity gradually after each use, and retained almost 54% of the initial activity after 15 uses. These results indicate that the immobilized enzyme could be used for industrial applications. The sodium-alginate- $\beta$ -cyclodextrin immobilized mannanase retained more than 70% of activity after 15 repeated cycles [12]. Laccase immobilized on  $\text{SiO}_2$  nanoparticles retained 94% of its initial activity after 5 cycles of repeated use, and 83% activity after 10 cycles [55]. The decrease in the enzyme activity may be due to the denaturation of bonds, as well as because of the enzyme leakage [28].

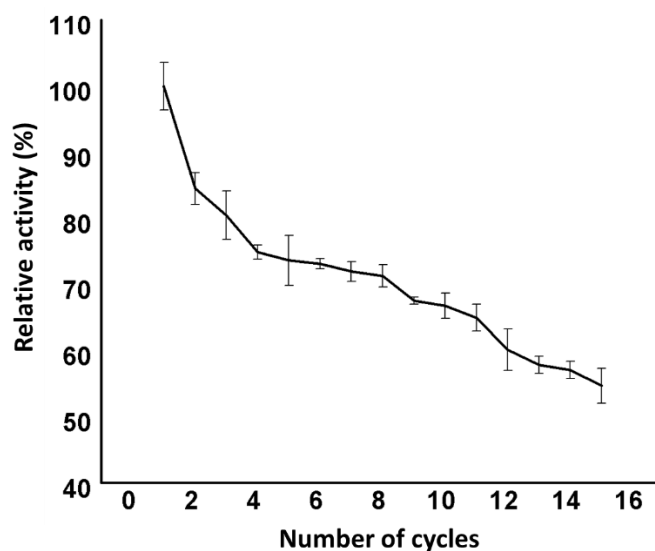


**Figure 8.** Reusability of the immobilized Man/Cel5B.

### 3.4. Fourier-Transform Infrared Spectroscopy (FTIR) Spectrum of Chitosan and Chitosan Immobilized Beads

FTIR analysis was performed to illustrate the functional groups present in the glutaraldehyde reinforced chitosan beads and Man/Cel5B immobilized beads (Figure 9). The main peaks for glutaraldehyde reinforced chitosan beads can be assigned as follows:  $1022\text{ cm}^{-1}$ ,  $71\text{ cm}^{-1}$  (C-OH stretching vibration),  $1149\text{ cm}^{-1}$  (monosaccharide structure present in chitosan polymer),  $1427\text{ cm}^{-1}$  (C-N stretching vibration),  $1583\text{ cm}^{-1}$  (N-H bond), and  $3293\text{ cm}^{-1}$  (N-H and O-H stretching vibration) [56]. In addition to this, the band at  $1775\text{ cm}^{-1}$  maybe because of the CHO group present in glutaraldehyde [55]. Nevertheless, some major changes were observed in the FTIR spectrum of Man/Cel5B immobilized chitosan beads when compared to the FTIR spectrum of glutaraldehyde reinforced chitosan beads. The FTIR spectrum of Man/Cel5B immobilized chitosan beads reveals that the N-H and O-H stretching vibration at  $3293\text{ cm}^{-1}$  shifts to  $3292\text{ cm}^{-1}$ . The appearance of band at  $1410.10\text{ cm}^{-1}$  could be attributed to CH stretching vibration of  $\beta$ -mannanase [55]. Moreover, the band at  $1563.05\text{ cm}^{-1}$  could be attributed to the N-H bending vibration of the amide II. These results also agree with the immobilization of  $\beta$ -galactosidase on chitosan, and cellulase on chitosan magnetic nanoparticles [57].

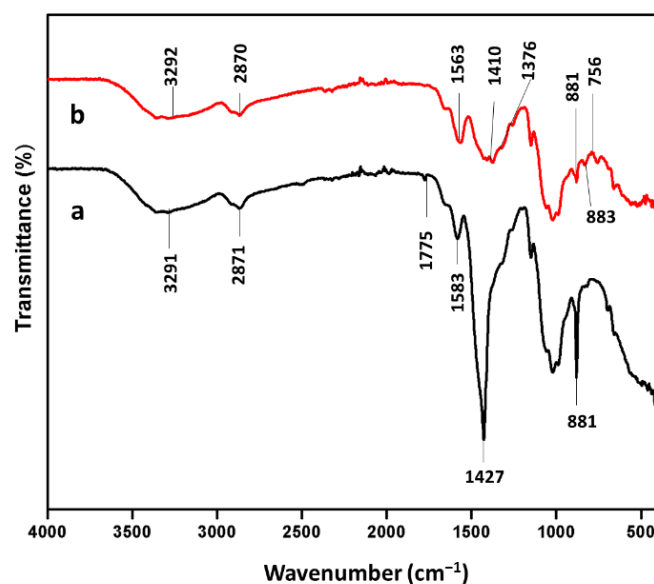


**Figure 9.** FTIR spectra of chitosan beads and Man/Cel5B immobilized chitosan beads. (a) Chitosan beads. (b) Immobilized chitosan beads.

### 3.5. X-ray Powder Diffraction (XRD) of Chitosan and Chitosan Immobilized Beads

The change in the crystal structure of chitosan beads before and after immobilization of Man/Cel5B was investigated using XRD. The XRD is a useful tool to study crystal lattice arrangements and provides valuable information about the degree of crystallinity in the sample. The XRD patterns of chitosan beads and Man/Cel5B-immobilized chitosan beads are shown in Figure 10. The XRD pattern of chitosan beads depicted a broad diffraction peak at  $2\theta = 20^\circ$ , which is the characteristic peak for crystal chitosan. The additional peaks were observed at  $2\theta = 30^\circ$ ,  $35^\circ$ , and  $38^\circ$  of Man/Cel5B immobilized chitosan beads. The appearance of new peaks confirms the strong binding of chitosan beads with the Man/Cel5B beads.



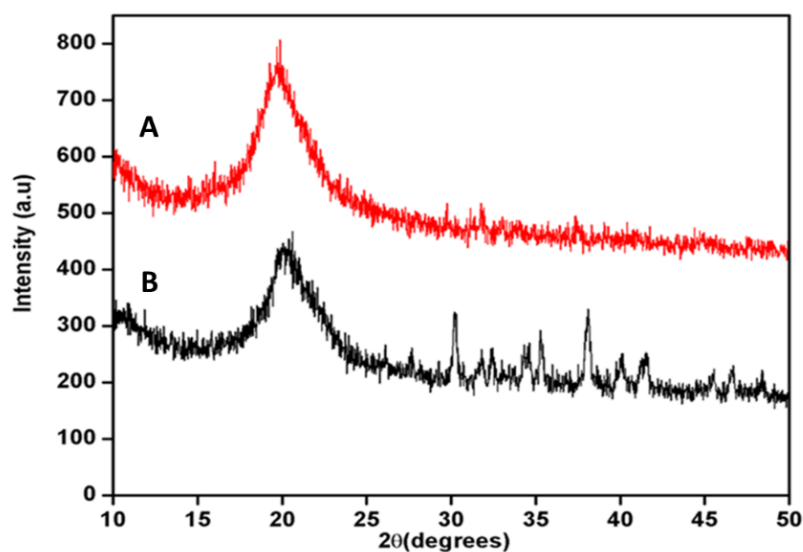


**Figure 10.** XRD spectra of chitosan beads and Man/Cel5B immobilized beads. (A) Chitosan beads. (B) Man/Cel5B immobilized chitosan beads.

### 3.6. Molecular Docking Analysis

The Psi Ramachandra plot obtained from PROCHECK analysis displayed that 88.20% amino acid residues of Man/Cel5B reside in the most favored region, and 11.80% of amino acid residues in additional allowed regions and no amino acid residue were found in generously allowed or disallowed regions (Figure S1). Further Verify-3D analysis was carried out to check the quality of the predicted mannanase structure. The Verify-3D depicted that the average 3D-ID score of 97.54% of the amino acid residues predicted model of Man/Cel5B is  $>0.2$  which strongly indicates that the predicted structure is of adequate quality. The CASTp analysis showed that the amino acid residues such as Phe17, His86, Val93, Asn94, Lys95, Glu139, Phe142, Gly179, Tyr180, Asn182, Tyr200, Ile201, Phe203, His207, Trp212, Val213, His229, Glu259, Trp292, and Phe298 might play an important role at catalytic site (Figure S2). The molecular docking analysis revealed that the Man/Cel5B structure has strong hydrogen-bonding interactions with the mannotriose ligand (Figure 11). The docked complex showed that there are strong hydrogen-bonding interactions between Man/Cel5B active site residue His86 and mannotriose (BMA 1.C O6) by interatomic distance of 2.6 Å (Figure 12A,B; Table 3). Similarly, Glu 139 (A OE1) interacts with mannotriose (BMA 2.C C1:) by interatomic distance of 2.7 Å. Additionally, the docked complex showed strong hydrogen-bonding of active site residues such as Tyr180, Asn182, His207, Trp212, Glu259, and Trp292 with mannotriose. Hence from this docking of  $\beta$ -mannanase with mannotriose showed very strong hydrogen-bonding interactions with mannotriose ligand.

**Table 3.** Hydrogen-bonding interactions between mannanase with mannotriose.

Sr. No.	Interaction between Amino Acid Residues of Mannanase with Mannotriose	Distance in Å
1	BMA 1.C O5 — TRP 292.A CZ2:	3.302
2	HIS 86.A NE2 — BMA 1.C O6:	2.645
3	ASN 138.A ND2 — BMA 1.C O6:	3.473
4	BMA 1.C C6 — GLU 259.A OE1:	3.319
5	TRP 212.A NE1 — BMA 1.C O3:	1.243
6	BMA 2.C O2 — HIS 207.A NE2:	3.039

Table 3. Cont.

Sr. No.	Interaction between Amino Acid Residues of Mannanase with Mannotriose	Distance in Å
7	GLU 139.A OE1 — BMA 2.C C1:	2.769
8	TYR 180.A CE2 — BMA 3.C O2:	1.721
9	ASN 182.A OD1 — BMA 3.C O6:	2.344

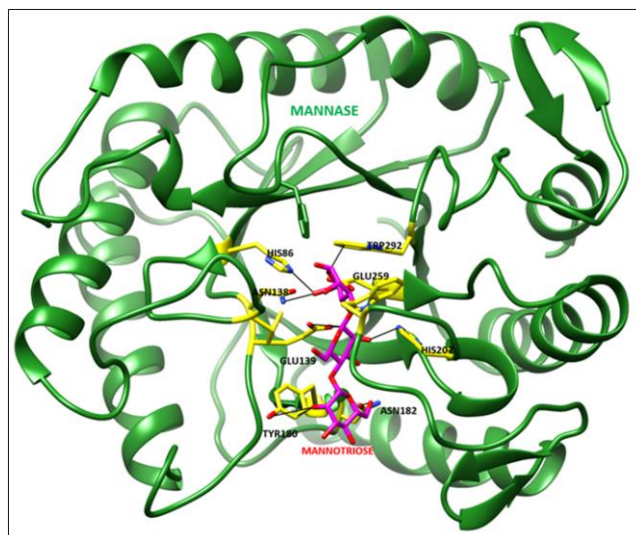


Figure 11. Docked complex of Mannanase (Green) with Mannotriose (Magenta).

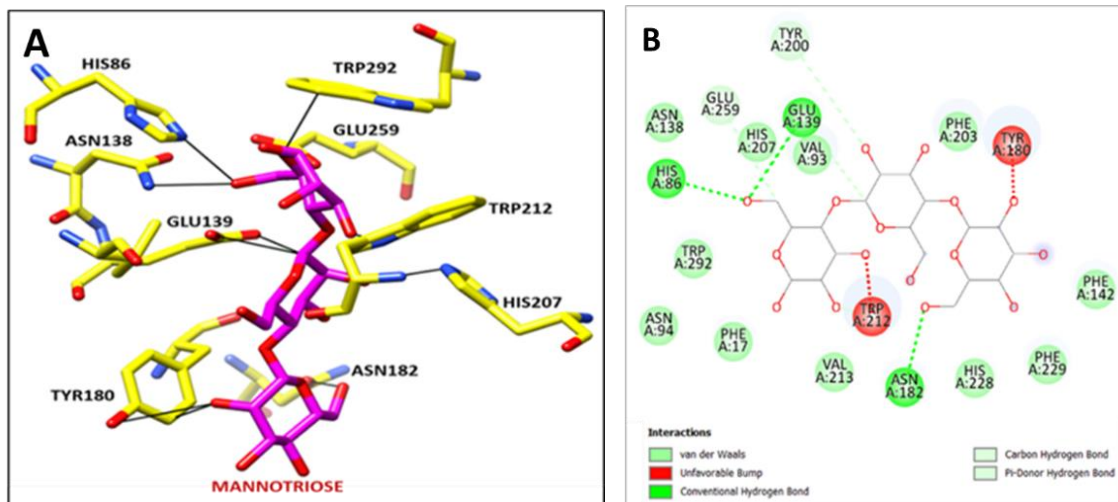


Figure 12. (A) Bonding interaction of active site residues of Mannanase (yellow) with Mannotriose (Magenta). (B) 2D-interactions between active site residues of mannanase with mannotriose.

#### 4. Conclusions

The purified Man/Cel5B was successfully immobilized on glutaraldehyde cross-linked chitosan beads with an immobilization yield of 71.8%. The immobilized enzyme depicted its optimal activity at pH 5.5 and 95 °C compared to pH 5.5 and 85 °C for the free enzyme. The immobilized enzyme revealed better thermodynamic properties compared to the soluble enzyme which is an essential feature for possible industrial use of  $\beta$ -mannanase. The substrate affinity for LBG of the immobilized enzyme complex was higher than the soluble enzyme. All these features make chitosan immobilized Man/Cel5B an promising candidate for many biotechnological applications.

**Supplementary Materials:** The following supporting information can be downloaded at: <https://www.mdpi.com/article/10.3390/biom12070999/s1>, Figure S1: Ramachandran Plot of Man/Cel5B structure; Figure S2: Structural validation using Verify-3D 3D/1D profile; Figure S3: Active site prediction for Man/Cel5B structure using CASTp server.

**Author Contributions:** Conceptualization, Y.S., W.S. and B.S.; Methodology, B.S. and M.A.D.; Software, M.J.D., K.D.S. and B.S.; Validation, B.S., C.S. and H.M.; Writing—Original draft preparation, B.S.; Writing—Review and editing, M.A.D. and H.M.; Supervision, Y.S. and W.S.; Funding acquisition, Y.S. and W.S. All authors have read and agreed to the published version of the manuscript.

**Funding:** This work was supported by National Natural Science Foundation of China (Grant No. 31770089, 31972851 and 31670064), and Advanced Talent Research Fund Project of Jiangsu University (16JDG031).

**Institutional Review Board Statement:** Not applicable.

**Informed Consent Statement:** Not applicable.

**Data Availability Statement:** Not applicable.

**Acknowledgments:** B.S. acknowledges Shandong University of Technology for postdoctoral fellowship.

**Conflicts of Interest:** The authors declare no conflict of interest.

## References

- Scheller, H.V.; Ulvskov, P. Hemicelluloses. *Annu. Rev. Plant Biol.* **2010**, *61*, 263–289. [[CrossRef](#)] [[PubMed](#)]
- Chauhan, P.S.; Puri, N.; Sharma, P.; Gupta, N. Mannanases: Microbial sources, production, properties and potential biotechnological applications. *Appl. Microbiol. Biotechnol.* **2012**, *93*, 1817–1830. [[CrossRef](#)] [[PubMed](#)]
- Albuquerque, D.; Costa, L.; Ximenes, E.; Filho, F. Microbial  $\beta$ -mannosidases and their industrial applications. *Appl. Microbiol. Biotechnol.* **2018**, *103*, 535–547.
- Lesage, G.; Bussey, H. Cell Wall Assembly in *Saccharomyces cerevisiae*. *Microbiol. Mol. Biol. Rev.* **2006**, *70*, 317–343. [[CrossRef](#)] [[PubMed](#)]
- Liu, W.; Tu, T.; Gu, Y.; Wang, Y.; Zheng, F.; Zheng, J.; Wang, Y.; Su, X.; Yao, B.; Luo, H. Insight into the Thermophilic Mechanism of a Glycoside Hydrolase Family 5  $\beta$ -Mannanase. *J. Agric. Food Chem.* **2019**, *67*, 473–483. [[CrossRef](#)]
- Sadaqat, B.; Sha, C.; Rupani, P.F.; Wang, V.; Zuo, W.; Shao, W. Man/Cel5B, a Bifunctional Enzyme Having the Highest Mannanase Activity in the Hyperthermic Environment. *Front. Bioeng. Biotechnol.* **2021**, *9*, 637649. [[CrossRef](#)]
- Dawood, A.; Ma, K. Applications of microbial  $\beta$ -mannanases. *Front. Bioeng. Biotechnol.* **2020**, *8*, 598630. [[CrossRef](#)]
- Mohapatra, B.R. Characterization of  $\beta$ -mannanase extracted from a novel *Streptomyces* species Alg-S25 immobilized on chitosan nanoparticles. *Biotechnol. Biotechnol. Equip.* **2021**, *35*, 150–161. [[CrossRef](#)]
- Boudrant, J.; Woodley, J.M.; Fernandez-Lafuente, R. Parameters necessary to define an immobilized enzyme preparation. *Process Biochem.* **2020**, *90*, 66–80. [[CrossRef](#)]
- Lopes, L.A.; Dias, L.P.; da Costa, H.P.S.; da Silva Neto, J.X.; Morais, E.G.; de Oliveira, J.T.A.; Vasconcelos, I.M.; de Sousa, D.D.O.B. Immobilization of a peroxidase from *Moringa oleifera* Lam. roots (MoPOX) on chitosan beads enhanced the decolorization of textile dyes. *Process Biochem.* **2021**, *110*, 129–141. [[CrossRef](#)]
- Homaei, A.A.; Sariri, R.; Vianello, F.; Stevanato, R. Enzyme immobilization: An update. *J. Chem. Biol.* **2013**, *6*, 185–205. [[CrossRef](#)] [[PubMed](#)]
- Dhiman, S.; Srivastava, B.; Singh, G.; Khatri, M.; Arya, S.K. Immobilization of mannanase on sodium alginate-grafted- $\beta$ -cyclodextrin: An easy and cost-effective approach for the improvement of enzyme properties. *Int. J. Biol. Macromol.* **2020**, *156*, 1347–1358. [[CrossRef](#)] [[PubMed](#)]
- Panwar, D.; Kaira, G.S.; Kapoor, M. Cross-linked enzyme aggregates (CLEAs) and magnetic nanocomposite grafted CLEAs of GH26 endo- $\beta$ -1,4-mannanase: Improved activity, stability and reusability. *Int. J. Biol. Macromol.* **2017**, *105*, 1289–1299. [[CrossRef](#)] [[PubMed](#)]
- Behera, S.; Dev, M.J.; Singhal, R.S. Cross-linked beta-Mannanase Aggregates: Preparation, Characterization, and Application for Producing Partially Hydrolyzed Guar Gum. *Appl. Biochem. Biotechnol.* **2022**, *194*, 1981–2004. [[CrossRef](#)] [[PubMed](#)]
- El-Naggar, M.Y.; El-Aassar, S.A.; Youssef, A.S.; El-Sersy, N.A.; Beltagy, E.A. Extracellular  $\beta$ -mannanase production by the immobilization of the locally isolated *Aspergillus niger*. *Int. J. Agric. Biol.* **2006**, *8*, 57–62.
- Seenuvasan, M.; Kumar, K.S.; Kumar, A.; Parthiban, R. Review on surface modification of nanocarriers to overcome diffusion limitations: An enzyme immobilization aspect. *Biochem. Eng. J.* **2020**, *158*, 107574.
- Machado, N.B.; Miguez, J.P.; Bolina, I.C.; Salviano, A.B.; Gomes, R.A.; Tavano, O.L.; Luiz, J.H.H.; Tardioli, P.W.; Cren, E.C.; Mendes, A.A. Preparation, functionalization and characterization of rice husk silica for lipase immobilization via adsorption. *Enzym. Microb. Technol.* **2019**, *128*, 9–21. [[CrossRef](#)]

18. Nunes, Y.L.; de Menezes, F.L.; de Sousa, I.G.; Cavalcante, A.L.G.; Cavalcante, F.T.T.; da Silva Moreira, K.; de Oliveira, A.L.B.; Mota, G.F.; Souza, J.E.D.S.; Falcão, I.R.D.A.; et al. Chemical and physical Chitosan modification for designing enzymatic industrial biocatalysts: How to choose the best strategy? *Int. J. Biol. Macromol.* **2021**, *181*, 1124–1170. [[CrossRef](#)]
19. Mo, H.; Qiu, J.; Yang, C.; Zang, L.; Sakai, E.; Chen, J. Porous biochar/chitosan composites for high performance cellulase immobilization by glutaraldehyde. *Enzym. Microb. Technol.* **2020**, *138*, 109561. [[CrossRef](#)]
20. Suryawanshi, R.K.; Jana, U.K.; Prajapati, B.P.; Kango, N. Immobilization of *Aspergillus quadrilineatus* RSNK-1 multi-enzymatic system for fruit juice treatment and manno oligosaccharide generation. *Food Chem.* **2019**, *289*, 95–102. [[CrossRef](#)]
21. Raharjo, T.J.; Febrina, L.; Wardoyo, F.A.; Swasono, R.T. Research Article Effect of Deacetylation Degree of Chitosan as Solid Support in Lipase Immobilization by Glutaraldehyde Crosslink. *J. Biochem.* **2016**, *11*, 127–134.
22. Işık, M. High stability of immobilized acetylcholinesterase on chitosan beads. *ChemistrySelect* **2020**, *5*, 4623–4627. [[CrossRef](#)]
23. Kaushal, J.; Singh, G.; Arya, S.K. Immobilization of catalase onto chitosan and chitosan–bentonite complex: A comparative study. *Biotechnol. Rep.* **2018**, *18*, e00258. [[CrossRef](#)] [[PubMed](#)]
24. Hermanto, D.; Mudasir, M.; Siswanta, D.; Kuswandi, B.; Ismillayli, N. Polyelectrolyte Complex (PEC) of the Alginate-Chitosan Membrane for Immobilizing Urease. *J. Math. Fundam. Sci.* **2019**, *51*, 309–319. [[CrossRef](#)]
25. 27Lever, M. A new reaction for colorimetric determination of carbohydrates. *Anal. Biochem.* **1972**, *47*, 273–279.
26. Simonian, M.H. Spectrophotometric determination of protein concentration. *Curr. Protoc. Toxicol.* **2004**, *3*, 1–7. [[CrossRef](#)]
27. Schwede, T.; Kopp, J.; Guex, N.; Peitsch, M.C. SWISS-MODEL: An automated protein homology-modeling server. *Nucleic Acids Res.* **2003**, *31*, 3381–3385. [[CrossRef](#)]
28. Eisenberg, D.; Luthy, R.; Bowie, J.U. VERIFY3D: Assessment of protein models with three-dimensional profiles. *Methods Enzymol.* **1997**, *277*, 396–404.
29. Laskowaski, R.A.; McArthur, M.W.; Moss, D.S.; Thornton, J.M. PROCHECK a program to check stereo-chemical quality of a protein structures. *J. Appl. Crystallogr.* **1993**, *26*, 283–291. [[CrossRef](#)]
30. Pettersen, E.F.; Goddard, T.D.; Huang, C.C.; Couch, G.S.; Greenblatt, D.M.; Meng, E.C.; Ferrin, T.E. UCSF Chimera—A visualization system for exploratory research and analysis. *J. Comput. Chem.* **2004**, *25*, 1605–1612. [[CrossRef](#)]
31. D. Systèmes. *Discovery Studio Visualizer*; BIOVIA, Dassault Systèmes: San Diego, CA, USA, 2021.
32. Bao, Y.; Shao, L.; Xing, G.; Qi, C. Cobalt, nickel and iron embedded chitosan microparticles as efficient and reusable catalysts for Heck cross-coupling reactions. *Int. J. Biol. Macromol.* **2019**, *130*, 203–212. [[CrossRef](#)]
33. Kim, H.J.; Kim, A.R.; Jeon, S.J. Immobilization on chitosan of a thermophilic trehalose synthase from *Thermus thermophilus* HJ6. *J. Microbiol. Biotechnol.* **2010**, *20*, 513–517. [[PubMed](#)]
34. Dinçer, A.; Becerik, S.; Aydemir, T. Immobilization of tyrosinase on chitosan–clay composite beads. *Int. J. Biol. Macromol.* **2012**, *50*, 815–820. [[CrossRef](#)] [[PubMed](#)]
35. Pal, A.; Khanum, F. Covalent immobilization of xylanase on glutaraldehyde activated alginate beads using response surface methodology: Characterization of immobilized enzyme. *Process Biochem.* **2011**, *46*, 1315–1322. [[CrossRef](#)]
36. Tripathi, P.; Kumari, A.; Rath, P.; Kayastha, A.M. Immobilization of  $\alpha$ -amylase from mung beans (*Vigna radiata*) on Amberlite MB 150 and chitosan beads: A comparative study. *J. Mol. Catal. B Enzym.* **2007**, *49*, 69–74. [[CrossRef](#)]
37. Akkuş Çetinus, Ş.; Öztıp, H.N. Immobilization of catalase into chemically crosslinked chitosan beads. *Enzym. Microb. Technol.* **2003**, *32*, 889–894. [[CrossRef](#)]
38. Lin, K.P.; Feng, G.J.; Pu, F.L.; Hou, X.D.; Cao, S.L. Enhancing the Thermostability of Papain by Immobilizing on Deep Eutectic Solvents-Treated Chitosan With Optimal Microporous Structure and Catalytic Microenvironment. *Front. Bioeng. Biotechnol.* **2020**, *8*, 576266. [[CrossRef](#)]
39. Sohrabi, N.; Rasouli, N.; Torkzadeh, M. Enhanced stability and catalytic activity of immobilized  $\alpha$ -amylase on modified Fe<sub>3</sub>O<sub>4</sub> nanoparticles. *Chem. Eng. J.* **2014**, *240*, 426–433. [[CrossRef](#)]
40. Ahmed, S.A.; Mostafa, F.A.; Ouis, M.A. Enhancement stability and catalytic activity of immobilized  $\alpha$ -amylase using bioactive phospho-silicate glass as a novel inorganic support. *Int. J. Biol. Macromol.* **2018**, *112*, 371–382. [[CrossRef](#)]
41. Akkuş Çetinus, Ş.; Öztıp, H.N. Immobilization of catalase on chitosan film. *Enzyme Microb. Technol.* **2000**, *26*, 497–501. [[CrossRef](#)]
42. Shafei, M.S.; Allam, R.F. Production and immobilization of partially purified lipase from *Penicillium chrysogenum*. *Malays. J. Microbiol.* **2010**, *6*, 196–202.
43. Altun, G.D.; Cetinus, S.A. Immobilization of pepsin on chitosan beads. *Food Chem.* **2007**, *100*, 964–971. [[CrossRef](#)]
44. Riaz, M.; Perveen, R.; Javed, M.R.; Nadeem, H.; Rashid, M.H. Kinetic and thermodynamic properties of novel glucoamylase from *Humicola* sp. *Enzym. Microb. Technol.* **2007**, *41*, 558–564. [[CrossRef](#)]
45. Hameed, U.; Ul-Haq, I. Kinetics and thermodynamics of catalysis and thermal inactivation of a novel  $\alpha$ -amylase (Tp-AmyS) from *Thermotoga petrophila*. *Biocatal. Biotransform.* **2020**, *38*, 227–233. [[CrossRef](#)]
46. Guzik, U.; Hupert-Kocurek, K.; Wojcieszynska, D. Immobilization as a strategy for improving enzyme properties-application to oxidoreductases. *Molecules* **2014**, *19*, 8995–9018. [[CrossRef](#)] [[PubMed](#)]
47. dos Santos, E.A.L.; Lima, Á.S.; Soares, C.M.F.; de Aquino Santana, L.C.L. Lipase from *Aspergillus niger* obtained from mangaba residue fermentation: Biochemical characterization of free and immobilized enzymes on a sol-gel matrix. *Acta Scientiarum. Technol.* **2017**, *39*, 1–8. [[CrossRef](#)]
48. Sel, E.; Ulu, A.; Ateş, B.; Köytepe, S. Comparative study of catalase immobilization via adsorption on P (MMA-co-PEG500MA) structures as an effective polymer support. *Polym. Bull.* **2021**, *78*, 2663–2684. [[CrossRef](#)]

49. Zheng, F.; Cui, B.-K.; Wu, X.-J.; Meng, G.; Liu, H.-X.; Jing, S. Immobilization of laccase onto chitosan beads to enhance its capability to degrade synthetic dyes. *Int. Biodeterior.* **2016**, *110*, 69–78. [[CrossRef](#)]
50. Wehaidy, H.R.; Abdel-Naby, M.A.; El-Hennawi, H.M.; Youssef, H.F. Nanoporous Zeolite-X as a new carrier for laccase immobilization and its application in dyes decolorization. *Biocatal. Agric. Biotechnol.* **2019**, *19*, 101135. [[CrossRef](#)]
51. Worthen, A.J.; Irving, K.S.; Lapitsky, Y. Supramolecular strategy effects on chitosan bead stability in acidic media: A comparative study. *Gels* **2019**, *5*, 11. [[CrossRef](#)]
52. Wu, S.C.; Lia, Y.K. Application of bacterial cellulose pellets in enzyme immobilization. *J. Mol. Catal. B Enzym.* **2008**, *54*, 103–108. [[CrossRef](#)]
53. Blibech, M.; Chaari, F.; Bhiri, F.; Dammak, I.; Ghorbel, R.E.; Chaabouni, S.E. Production of manno-oligosaccharides from locust bean gum using immobilized *Penicillium occitanis* mannanase. *J. Mol. Catal. B Enzym.* **2011**, *73*, 111–115. [[CrossRef](#)]
54. Patel, S.K.; Kalia, V.C.; Choi, J.H.; Haw, J.R.; Kim, I.W.; Lee, J.K. Immobilization of laccase on  $\text{SiO}_2$  nanocarriers improves its stability and reusability. *J. Microbiol. Biotechnol.* **2014**, *24*, 639–647. [[CrossRef](#)] [[PubMed](#)]
55. Li, B.; Shan, C.L.; Zhou, Q.; Fang, Y.; Wang, Y.L.; Xu, F.; Han, L.; Ibrahim, M.; Guo, L.; Xie, G.; et al. Synthesis, characterization, and antibacterial activity of cross-linked chitosan-glutaraldehyde. *Mar. Drugs* **2013**, *11*, 1534–1552. [[CrossRef](#)]
56. Klein, M.P.; Nunes, M.R.; Rodrigues, R.C.; Benvenuti, E.V.; Costa, T.M.; Hertz, P.F.; Ninow, J.L. Effect of the support size on the properties of  $\beta$ -galactosidase immobilized on chitosan: Advantages and disadvantages of macro and nanoparticles. *Biomacromolecules* **2012**, *13*, 2456–2464. [[CrossRef](#)]
57. Chagas, P.M.B.; Caetano, A.A.; Tireli, A.A.; Cesar, P.H.S.; Corrêa, A.D.; do Rosário Guimarães, I. Use of an Environmental Pollutant from Hexavalent Chromium Removal as a Green Catalyst in The Fenton Process. *Sci. Rep.* **2019**, *9*, 1–15.